Published in final edited form as:

Nat Neurosci. 2010 March ; 13(3): 338–343. doi:10.1038/nn.2488.

A neuronal role for SNAP-23 in postsynaptic glutamate receptor trafficking

Young Ho Suh[1,2], **Akira Terashima**[3], **Ronald S. Petralia**[4], **Robert J. Wenthold**[4], **John T.R. Isaac**[3], **Katherine W. Roche**[1], and **Paul A. Roche**[2]

[1]Receptor Biology Section, National Institute of Neurological Disorders and Stroke, National Institutes of Health, Bethesda, MD 20892

[2]Experimental Immunology Branch, National Cancer Institute, National Institutes of Health, Bethesda, MD 20892

[3]Developmental Synaptic Plasticity Section, National Institute of Neurological Disorders and Stroke, National Institutes of Health, Bethesda, MD 20892

[4]National Institute on Deafness and Other Communication Disorders, National Institutes of Health, Bethesda, MD 20892

Abstract

Regulated exocytosis is essential for many biological processes, and many components of the protein trafficking machinery are ubiquitous. However, there are also exceptions such as SNAP-25, a neuron-specific SNARE protein, which is essential for synaptic vesicle release from presynaptic nerve terminals. In contrast, SNAP-23 is the ubiquitously-expressed SNAP-25 homologue that is critical for regulated exocytosis in non-neuronal cells. However, the role of SNAP-23 in neurons has not been elucidated. We now find that SNAP-23 is enriched in dendritic spines and colocalizes with constituents of the postsynaptic density, whereas SNAP-25 is restricted to axons. In addition, loss of SNAP-23 using genetically-altered mice or shRNA targeted to SNAP-23 leads to a dramatic decrease in NMDA receptor surface expression and NMDA receptor currents, whereas loss of SNAP-25 does not. Therefore SNAP-23 plays a unique role in the functional regulation of postsynaptic glutamate receptors.

Introduction

There has been intense interest in unraveling the molecular mechanisms underlying vesicle trafficking and fusion in neurons because membrane trafficking is essential to synaptic vesicle release1,2. For this reason, much of the protein machinery that regulates synaptic vesicle exocytosis has been defined. For example, a class of membrane-associated proteins termed SNAREs has been shown to regulate the process of synaptic vesicle fusion with the

Correspondence to: Paul A. Roche[2]paul.roche@nih.gov. Correspondence to: Katherine W. Roche[1]rochek@ninds.nih.gov.

Author Contributions

P.A.R and K.W.R. designed and supervised the experiments, and wrote the manuscript. Immunogold EM was performed by R.S.P. and R.J.W. Electrophysiology study was performed by A.T. and J.T.R.I. All other experiments were performed by Y.H.S.

presynaptic plasma membrane3,4. SNARE proteins on synaptic vesicles, such as synaptobrevin/VAMP, bind to SNAREs present on the presynaptic target membrane, forming a complex consisting of a four-helix bundle of coiled-coils that mediates synaptic vesicle-plasma membrane fusion. The synaptic vesicle SNARE synaptobrevin/VAMP contributes one coiled-coil to this complex, while on the plasma membrane the SNARE protein syntaxin provides an additional coiled-coil, and SNAP-25 provides two. There are extensive data highlighting the importance of each of these three classes of SNAREs in synaptic vesicle exocytosis from presynaptic terminals; however, it is unclear what precise role SNARE proteins play in regulating postsynaptic trafficking of neurotransmitter receptors.

SNAP-25 expression is limited to cells of neuronal and neuroendocrine lineage. Furthermore, there are many studies showing that SNAP-25 expression is limited to presynaptic membranes5-7 and functionally, SNAP-25 acts to regulate synaptic vesicle release8. Since the identification of the ubiquitously-expressed SNAP-25 homolog SNAP-239, many studies have shown that SNAP-23 regulates a wide variety of diverse membrane-membrane fusion events outside the CNS such as exocytosis from mast cells, insulin-dependent GLUT-4 release from adipocytes, and degranulation in platelets10-13. However, SNAP-23 is also expressed in brain14-16 and can functionally replace SNAP-25 in exocytosis from neuroendocrine cells17. Because SNAP-25 is expressed at a high level in brain and because binding studies have shown that SNAP-25 binds other SNARE-family members more efficiently than does SNAP-2313, it unclear why neurons would express both SNAP-23 and SNAP-25.

Synaptic transmission requires that secreted neurotransmitters bind to neurotransmitter receptors present on the postsynaptic membrane. Ionotropic glutamate receptors mediate most excitatory neurotransmission in the brain. NMDA receptors are a subtype of glutamate receptors that are widely distributed and play a crucial role in synaptic development, synaptic plasticity, and excitotoxicity18. Functional NMDA receptors are heteromeric combinations of the NR1 subunit with different NR2 subunits (NR2A-D)19. Although synaptic NMDA receptors are tightly anchored to the postsynaptic membrane via the postsynaptic density (PSD), they are also dynamic at the cell surface20. For example, NMDA receptors can undergo constitutive endocytosis to recycling endosomes21,22, vesicular exocytosis onto the plasma membrane18,23,24, and lateral diffusion between synaptic and extrasynaptic receptor pools20,25. Despite the extensive literature defining the molecular machinery regulating presynaptic neurotransmitter release, the proteins that control postsynaptic neurotransmitter receptor expression remain to be defined.

In this study, we show that while SNAP-25 is expressed exclusively in the axons of hippocampal neurons, the subcellular distribution of SNAP-23 is distinct and does not overlap with that of SNAP-25. SNAP-23 is expressed in both soma and dendrites and is highly enriched in postsynaptic spines. In addition, studies using shRNA and genetically-modified SNAP-23 heterozygous mice show that SNAP-23 regulates the surface expression and membrane recycling of NMDA receptors. Furthermore, whole-cell patch clamp recordings demonstrate that NMDA-evoked currents and NMDA EPSCs are also regulated

by SNAP-23. Taken together, this study reveals a novel role for SNAP-23 in the trafficking and functional regulation of postsynaptic glutamate receptors.

Results

SNAP-23 and SNAP-25 have distinct distributions in neurons

To address the role that SNAP-23 plays in regulating protein trafficking in neurons, we first examined the distribution of SNAP-23 and SNAP-25 in hippocampal neurons in culture using SNAP-23- or SNAP-25-specific antibodies (Fig. 1). After confirming the specificity of these antibodies on brain lysate or HeLa cell transfectants (Supplementary Fig. 1), we fixed and permeabilized cultured neurons (14–21 DIV) and double-labeled for total expression of SNAP-23 (green) and SNAP-25 (red) (Fig. 1a–c). We observed a completely distinct distribution of the two proteins, with SNAP-23 being localized to the somatodendritic compartment, whereas SNAP-25 was restricted to axons. Our data are in excellent agreement with previous electron microscopy studies showing that SNAP-25 is expressed almost exclusively on axons5-7. In contrast, SNAP-23 was present along MAP2 positive dendrites, and was heavily enriched in apparent dendritic spines (Fig. 1d). We observed almost no overlap in the distribution of these two related SNARE proteins.

We next analyzed the subcellular distribution of SNAP-23 and SNAP-25 using subcellular fractionation. We subjected homogenate of adult rat brain to differential centrifugation to purify distinct subcellular compartments. Both SNAP-23 and SNAP-25 were present in synaptic plasma membrane fractions (Fig. 1e) consistent with synaptic expression for both proteins. However, the two proteins were differentially expressed in the synaptic vesicle-enriched LP2 fraction. As expected, SNAP-25 and VAMP-2 were both present in the synaptic vesicle-enriched fraction. In contrast, the distribution of SNAP-23 more closely resembled that of PSD-95 and the NMDA receptor subunits, NR2A and NR2B, proteins that are highly enriched at postsynaptic sites (Fig. 1e).

In addition to examining the cellular distribution of SNAP-23 and SNAP-25, we also examined the developmental profile of these two proteins. SNAP-25 has been shown to be expressed at a low level from E15 and expression increases steadily through adulthood, with the most dramatic increase being observed between 3 and 8 weeks after birth26. Consistent with these reports, we found SNAP-25 expression to be low at P1 and gradually increase through P21 both in hippocampus and cortex. In contrast, SNAP-23 was expressed at similar levels at all times after birth in both hippocampus and cortex like the NMDA receptor subunits NR2B and NR1 (Fig. 1f). The distinct patterns of SNAP-23 and SNAP-25 expression in the brain are consistent with different roles for these two proteins in the nervous system.

SNAP-23 is localized to postsynaptic spines in neurons

We next investigated the subcellular distribution of SNAP-23 in dendrites and spines using both light microscopy and electron microscopy. We stained neurons for endogenous SNAP-23 and a variety of dendritic and postsynaptic markers. Consistent with our initial observation that SNAP-23 was expressed in punctate structures along dendrites, we found

that SNAP-23 was enriched in dendritic spines as visualized by F-actin staining (Fig. 2a). We also observed robust colocalization of SNAP-23 with PSD-95 (Fig. 2b) and Shank (Supplementary Fig. 2a), major constituents of the PSD. We observed closely apposed (but not colocalized) staining of SNAP-23 with the presynaptic SNARE proteins VAMP-2 (Fig. 2c) or synaptophysin (Supplementary Fig. 2b). We observed no colocalization of SNAP-23 with gephyrin (Fig. 2d), a marker of inhibitory synapses, thus revealing a striking specificity of SNAP-23 for excitatory synapses. Furthermore, SNAP-23 was highly co-localized with NMDA receptors and AMPA receptors (Fig. 2e and Supplementary Fig. 2c). The postsynaptic localization of SNAP-23 was confirmed by immunoelectron microscopy. SNAP-23 was expressed primarily at the PSD and at many synapses SNAP-23 had a perisynaptic localization (Fig. 2f). Thus SNAP-23 is co-expressed with NMDA receptors at excitatory synapses, but not inhibitory synapses.

Surface NMDA receptors are reduced in SNAP-23$^{+/-}$ mice

To analyze the functional role of postsynaptic SNAP-23 in vivo, we generated SNAP-23 deficient mice. Exon 2 of *Snap-23* was targeted for Cre-mediated excision because this is the first coding exon of the mouse *Snap-23* gene27. Embryonic stem cells harboring the targeted allele were generated by homologous recombination using the strategy outlined in Figure 3a and the generation of targeted mice from germ-line chimeras was confirmed using Southern blot analysis and genomic PCR (Fig. 3b,c). Mice lacking *Snap-23* exon 2 were generated by mating SNAP-23$^{fl/+}$ mice with transgenic mice expressing Cre under the control of the ubiquitous EIIa promoter. Viable SNAP-23 null mice were never obtained from SNAP-23 heterozygous matings and timed-pregnancy studies showed that SNAP-23 null embryos die prior to E3.5 (Suh *et al*., manuscript in preparation). Nevertheless, protein expression of SNAP-23 was reduced by half in SNAP-23 heterozygous mice (Fig. 3d), and we therefore utilized these mice to examine the role of SNAP-23 in regulating the expression of glutamate receptors. Total expression of NMDA and AMPA receptors from hippocampal P2 crude synaptosomes of 3-week-old mice was not significantly different between wild-type and SNAP-23 heterozygous mice (Fig. 3e). To examine the surface expression of glutamate receptors, we utilized a cell surface biotinylation assay in primary neuronal cultures derived from wild-type and SNAP-23 heterozygous mice. Surface expression of NMDA receptor subunits was significantly reduced in SNAP-23 heterozygous mice, with NR2B being more affected than NR1 (Fig. 3f,g). However, surface expression of the AMPA receptor subunits GluR1 and GluR2, the GABA(A) α1 receptor, or mGluR7, a presynaptic metabotropic glutamate receptor, was not significantly altered. These data demonstrate that reduced expression of endogenous SNAP-23 regulates the surface expression of NMDA receptors in neurons.

SNAP-23, not SNAP-25, regulates NMDA receptor expression

While our data show that SNAP-23 regulates NMDA receptor expression, they do not rule out the possibility that SNAP-25 also plays a similar role. To directly compare the role of SNAP-23 and SNAP-25, we generated lentivirus harboring shRNA to knock-down either endogenous SNAP-23 or endogenous SNAP-25 in neurons. Among three different targets to knock-down SNAP-23, SNAP-23 202 shRNA was the most effective (Supplementary Fig. 3). This target shRNA sequence was therefore used throughout this study. For SNAP-25, a

previously described target shRNA sequence was utilized28. Each shRNA inhibited expression of its specific target by >90% as determined by quantitative densitometry of SNAP-23 and SNAP-25 immunoblots. We evaluated the surface expression of NMDA and AMPA receptors and found that knock-down of endogenous SNAP-23 resulted in a significant decrease in the surface-expressed NMDA receptor subunits NR2A, NR2B, and NR1. This pronounced decrease in NMDA receptor surface expression was in contrast to the modest decrease in surface expression of the AMPA receptor subunits GluR1 and GluR2. The changes in surface expression of glutamate receptors were specific to SNAP-23, because knock-down of SNAP-25 did not have any effect on the surface expression of NMDA or AMPA receptor subunits (Fig. 4). However, surface expression of mGluR7, mGluR5, or GABA(A) α1 receptors was not significantly altered (Supplementary Fig. 4). Furthermore, SNAP-23 knock-down did not alter the total expression of any of these receptors under our viral transduction conditions, demonstrating that the observed effects were specific for the expression of each protein at the cell surface.

SNAP-23 regulates NMDA receptor recycling in neurons

The change in surface expression of NMDA receptors could be the result of either enhanced endocytosis or impaired exocytosis of these receptors. Because NR2B-containing NMDA receptors have been demonstrated to recycle robustly22,24,29, we performed endocytosis and recycling assays of NR2B containing an extracellular GFP tag to allow labeling of surface-expressed receptors. We transduced hippocampal neurons with lentivirus containing shRNA of SNAP-23 for 5–6 days, and transfected the cells with GFP-NR2B. There was no significant change of NR2B endocytosis by SNAP-23 knock-down (Fig. 5a,c). However, a recycling assay revealed that SNAP-23 knock-down inhibited the exocytosis of internalized NR2B back to the plasma membrane (Fig. 5b,d and Supplementary Fig. 5). These data demonstrate that the decreased expression of NMDA receptors on the surface of neurons lacking SNAP-23 is due to impaired receptor recycling and reveal that SNAP-23 expression at postsynaptic excitatory synapses regulates NMDA receptor expression.

SNAP-23 regulates NMDA-evoked currents and NMDA EPSCs

To investigate the functional effects of SNAP-23, we measured NMDA receptor-mediated currents in hippocampal CA1 pyramidal neurons following knock-down of SNAP-23. After 7–10 days of shRNA lentivirus knock-down we electrophysiologically assayed the total amount of NMDA receptors on the surface of CA1 pyramidal neurons using whole-cell voltage clamp recordings. Cells were voltage-clamped at a membrane potential of −40 mV and NMDA was bath-applied for 5 minutes, which produced a large slow inward current. In cells expressing SNAP-23 shRNA this current was significantly reduced as compared to cells expressing scrambled shRNA (Fig. 6a). Furthermore, SNAP-25 shRNA had no effect on the size of the NMDA-evoked current, consistent with SNAP-23, but not SNAP-25, regulating the number of NMDA receptors on the cell surface.

To address whether SNAP-23 specifically affects the number of receptors expressed at synapses, we recorded NMDA receptor-mediated excitatory postsynaptic currents (EPSCs) at a holding potential of +40 mV. We compared the amplitude of the NMDA EPSCs between cells expressing SNAP-23 shRNA and in-slice uninfected control cells using the

same stimulation position and stimulus intensity. NMDA EPSCs in SNAP-23 shRNA-expressing neurons were significantly smaller than those in the control cells (Fig. 6b) demonstrating that SNAP-23 also regulates the number of the NMDA receptors at CA1 synapses.

Discussion

SNARE proteins mediate membrane-membrane fusion events between distinct intracellular organelles in all cell types2-4. Many different SNAREs have been identified, and in some cases a role for a particular SNARE in a defined membrane fusion event has been defined. For example, SNAP-25 is a neuron-specific SNARE that regulates synaptic vesicle fusion with the presynaptic plasma membrane2-4,6,30. Curiously, there is a ubiquitously-expressed homolog of SNAP-25, termed SNAP-23, that is present in the brain but whose neuronal role in membrane fusion events has not been elucidated. We now show that SNAP-23 and SNAP-25 have unique and non-overlapping distributions and functions in neurons. Our own immunofluorescence studies, together with previous electron microscopy studies, show that SNAP-25 is localized on the presynaptic plasma membrane as well as on synaptic vesicles recycled from this membrane5-7. In marked contrast, SNAP-23 expression is somato-dendritic. Furthermore, immunofluorescence microscopy, electron microscopy, and subcellular fractionation studies show that SNAP-23 is localized at synaptic spines, and particularly enriched at the PSD.

The exclusive localization of SNAP-23 on dendrites supports a role for SNAP-23 in postsynaptic membrane trafficking events. Whereas previous studies have shown that ablation of SNAP-25 prevents stimulus-evoked neurotransmission8, our studies using knock-down of SNAP-25 expression with shRNA revealed no postsynaptic role for SNAP-25 in regulating glutamate receptors. By contrast, whole cell patch clamp recording in CA1 pyramidal neurons clearly shows that postsynaptic knock-down of SNAP-23, but not SNAP-25, reduced the size of NMDA-evoked currents, suggesting the number of NMDA receptors on the neuronal surface is regulated by SNAP-23. Furthermore, examination of NMDA EPSCs revealed that SNAP-23 regulates synaptic NMDA receptors, supporting our biochemical analyses and highlighting the physiological relevance of this work.

Our data reveal that SNAP-23 knock-down suppressed plasma membrane expression of NR2B by inhibiting the recycling of internalized receptors. This finding is consistent with previous studies showing that SNAP-23 is required for transferrin recycling in polarized epithelial cells31 and suggests that SNAP-23 may be a general regulator of membrane protein recycling. Our findings that NMDA receptors do not interact directly with SNAP-23 (Supplementary Fig. 6) are consistent with a more general role for SNAP-23 acting as a component of the membrane fusion machinery. Our hypothesis is that recycling endosomal compartments containing postsynaptic glutamate receptors are delivered to the plasma membrane and that membrane-bound SNARE proteins promote membrane fusion. While the precise nature of this postsynaptic plasma membrane SNARE complex remains to be determined, these data have identified SNAP-23 as a key player in this process.

SNARE-dependent exocytosis of glutamate receptors has been implicated in several studies. For example, the surface expression of AMPA receptors is regulated by the interaction of the AMPA receptor GluR2 subunit with NSF (N-ethylmaleimide-sensitive factor) and SNAPs (soluble NSF-attachment proteins), proteins that play a role in SNARE complex disassembly32-35. In addition, surface expression of NMDA receptors is increased upon activation of protein kinase C or mGluR1 and this effect is dependent on SNAP-2536,37. Finally, it has been demonstrated that SNARE cleavage by exogenously added clostridial neurotoxins can affect glutamate receptor expression24,32,36-39. However, SNARE-dependent trafficking of postsynaptic glutamate receptors that is attributed to SNAP-25 should be carefully evaluated. First, SNAP-25 is expressed at very low levels (if at all) on postsynaptic spines5-7, whereas the SNAP-25 homolog SNAP-23 is enriched at postsynaptic sites. Second, SNAP-25 has a much higher affinity than SNAP-23 for other SNAREs13, and thus overexpression of wild-type (or mutant) forms of SNAP-25 will also inhibit SNAP-23-dependent SNARE interactions. Third, infusion of small SNAP-25-derived blocking peptides to inhibit the formation of SNARE complexes will also likely inhibit SNAP-23 function because these two proteins share considerable amino acid identity9,27. Finally, even the use of clostridial neurotoxins to identify a role for particular SNARE proteins in neuronal function must be interpreted with caution, since these toxins generally cleave only free, and not complexed, SNAREs40. It is quite possible, therefore, that studies reporting the regulation of postsynaptic glutamate receptor expression by SNAP-25 may actually reflect effects on endogenous SNAP-23.

In conclusion, our findings reveal a distinct molecular composition of SNARE complexes at pre- and postsynaptic sites in neurons. The effects of SNAP-23 depletion on postsynaptic, but not presynaptic, glutamate receptor expression is consistent with the highly enriched localization of SNAP-23 to the PSD along dendritic spines. The reason for such a distinction between axonal and dendritic membrane fusion is fascinating and important topic for future study. Our work reveals a clear division of labor between SNAP-25 and neuronal SNAP-23 and supports a central role for SNAP-23 in postsynaptic trafficking events.

Methods

Antibodies

SNAP-23 antibody was raised in rabbits against a synthetic peptide Ac-MDDLSPEEIQLRAHQVC-amide corresponding to amino acids 1–16 of rat SNAP-23. Rabbit sera were collected and affinity-purified using the immobilized antigenic peptide (Quality Controlled Biochemicals, Hopkinton, MA). The following antibodies were purchased from commercial sources: PSD-95 6G6-1C9, GluR2 6C4 and polyclonal, GluR1 polyclonal, NR1 54.1, NR2A polyclonal, mGluR7a polyclonal (Millipore Corporation, Billerica, MA); NR1 R1JHL (Affinity BioReagents, Golden, CO); Synaptophysin SVP-38, microtubule-associated protein 2 (MAP2) HM-2, alpha-tubulin (Sigma, St. Louis, MO); pan-Shank N23B/49 (NeuroMab, Davis, CA); SNAP-25 SMI 81 (Covance, Berkeley, CA); Synaptobrevin2/VAMP-2 69.1, Gephyrin mAb7a (Synaptic Systems, Göttingen, Germany), GABA(A) α1 (Alomone Labs Ltd, Jerusalem, Israel). GFP rabbit polyclonal antibody and

all secondary antibodies for immunofluorescence were obtained from Invitrogen (Carlsbad, CA).

Immunocytochemistry

Primary hippocampal neurons were prepared from E18 Sprague-Dawley rats (Harlan, Indianapolis, IN) and grown in serum-free Neurobasal media (Invitrogen) with glutamine and B-27 supplement. All animal procedures used in this study were conducted according to the guidelines of the National Institutes of Health Animal Care and Use Committee. After 2–3 weeks in culture, hippocampal neurons were washed and fixed with 4% paraformaldehyde/4% sucrose in PBS for 15 min. For NR1 co-staining, hippocampal neurons were fixed in cold methanol for 20 min at −20°C. Neurons were permeabilized with 0.2% Triton X-100 for 5 min and incubated with 10% normal goat serum for 1 hr. Neurons were then incubated overnight at 4 °C with primary antibodies in 3% normal goat serum (NGS) as the following dilutions: SNAP-25 (SMI 81, 1:2000), SNAP-23 (1:500), MAP2 (HM-2, 1:500), PSD-95 (6G6-1C9, 1:500), Synaptobrevin2/VAMP-2 (69.1, 1:1000), Gephyrin (mAb7a, 1:250), NR1 (54.1, 1: 500), Shank (N23B/49, 1:200), Synaptophysin (SVP-38, 1:200), GluR2 (6C4, 1: 500). The neurons were washed and incubated for 30 min with Alexa Fluor 488 and/or 568- conjugated secondary antibodies. Phalloidin-Alexa Fluor 488 (1:50; Invitrogen) was used to label filamentous actin (F-actin). The neurons were washed and mounted (ProLong Antifade Kit, Invitrogen) and imaged with a 63 × Plan-Apochromat oil immersion objective [numerical aperture (NA)=1.4] on a Zeiss LSM 510 confocal microscope (Carl Zeiss MicroImaging, Inc., Thornwood, NY) equipped with 488 nm argon and 543 nm helium/neon lasers. Detection filters were band-pass 505–530 nm or long pass 560 nm for green or red channel, respectively. The pinhole aperture was set at less than 0.8 mm of optical slice. Serial optical sections collected at 0.36 μm intervals were used to create maximum projection images shown.

Immunogold electron microscopy

Postembedding immunogold labeling utilized established methods41-44. Briefly, rats were perfused with 4% paraformaldehyde + 0.5% glutaraldehyde, and sections were cryoprotected and frozen in a Leica EM CPC (Vienna, Austria), and embedded with Lowicryl HM-20 resin in a Leica AFS freeze-substitution instrument. Thin sections from 2 adult rats were incubated in 0.1% sodium borohydride + 50 mM glycine/Tris-buffered saline + 0.1% Triton X-100 (TBST), followed by 10% NGS in TBST, primary antibody in 1% NGS/TBST overnight, and then 10 nm immunogold labeling in 1% NGS in TBST + 0.5% polyethylene glycol (20,000 MW). Finally, sections were stained with uranyl acetate/lead citrate. Corresponding controls that lacked primary antibody showed only rare gold particles. Images were stored in their original formats and final images for figures were prepared in Adobe Photoshop: levels and brightness/contrast of images were minimally adjusted, evenly over the entire micrograph.

Subcellular fractionation

Subcellular fractionation was performed from thirty-day-old (P30) Sprague-Dawley rat brain as described previously45. Whole brain was homogenized to 10% (wt/vol) in ice cold 0.32 M sucrose buffer [0.32 M sucrose, 20 mM HEPES, pH 7.4, 5 mM EDTA, complete protease

inhibitor (Roche, Indianapolis, IN)] using 20 strokes with a glass homogenizer. The homogenate was spun at 800 × g for 10 min at 4 °C to remove the nuclear pellet (P1), and the supernatant (S1) was collected and then centrifuged at 9,200 × g for 15 min. The resulting pellet was washed once in 0.32 M sucrose buffer and recovered by spinning at 10,000 × g for 20 min (P2). The supernatant was further spun at 12,000 × g for 30 min to collect the supernatant (S2). S2 supernatant fraction was centrifuged at 165,000 × g for 2 hours at 4°C to yield the cytosolic supernatant (S3) and the microsomal pellet (P3). The P2 pellet (crude synaptosome) was resuspended in sucrose buffer and lysed by hypoosmotic shock using 9 volumes of H_2O and 3 strokes with a glass homogenizer, and rapidly adjusted to 7.5 mM HEPES (pH 7.4) and kept on ice for 30 min. The lysate was centrifuged at 25,000 × g for 20 min at 4 °C to yield the synaptosomal membrane pellet (LP1) and the supernatant (LS1). The supernatant LS1 was further spun at 165,000 × g for 2 hours at 4 °C to yield the synaptic cytosolic supernatant (LS2) and the synaptic vesicular pellet (LP2). The LP1 pellet was resuspended and layered on a discontinuous sucrose gradient containing 1.2 M, 1 M, and 0.8 M sucrose. The gradient was centrifuged at 150,000 × g for 2 hours at 4 °C, and the cloudy band between 1.2 M and 1 M sucrose was recovered and diluted to 0.32 M sucrose buffer. The diluted suspension was centrifuged at 150,000 × g for 30 min to yield the synaptic plasma membrane fraction (SPM).

Generation of SNAP-23 knock out mice

To generate the targeting construct, a BAC clone derived from 129 mouse genomic library harboring the entire SNAP-23 gene was used27. A neomycin resistance cassette containing the PGK promoter flanked by loxP sequences was inserted into XbaI/SpeI site at the 318 bp upstream of exon 2 which is also flanked by loxP. The thymidine kinase (HSV-tk) gene was cloned into EcoRI outside of 4.9 kb long arm sequences for double selection. The vector was electroporated into embryonic stem cells and colonies were selected in the presence of G418 and ganciclovir, and analyzed for homologous recombination by Southern blotting both with outside 5′ and 3′ probes. ES clones harboring targeted alleles were injected into blastocysts of C57BL/6J strain mice to generate germ-line chimeric offspring, which were further bred to generate targeted heterozygous mice. To generate SNAP-23 deficient mice, targeted heterozygous mice were mated with EIIa-Cre transgenic mice (in which Cre recombinase is highly expressed in gonads). Genotyping to screen the deletion of exon 2 was carried out using PCR as following primers; forward primer: 5′-TGCCCATAGGTTGTCAGACT-3′, reverse primer 1 : 5′-ATGTGCTAACCATGACCTTGA-3′, reverse primer 2 : 5′-GAGAGACCTCAGATGGTGGAG-3′.

Virus preparation and infection

To specifically knock down SNAP-23 or SNAP-25 in neurons, modified FUGW lentivirus vector harboring a short shRNA hairpin sequence was utilized as previously described46. A short hairpin targeting the rat SNAP-23 sequence (GAGGCAGAGAAGACUUUAA) or rat SNAP-25 sequence (GUUGGAUGAGCAAGGCGAA)28 was cloned under H1 promoter cassette of pSuper vector (OligoEngine, WA), and then H1-shRNA sequence was cloned between the HIV-flap and ubiquitin promoter of FUGW vector (kindly provided by Dr. Robert C. Malenka). EGFP is expressed under a ubiquitin promoter to monitor the virus production and infection. For the production of lentivirus, the lentiviral vector harboring

shRNA sequence, the packaging vector Δ8.9, and the VSVG envelope glycoprotein vector were co-transfected into HEK-293FT cells using FUGENE6 reagent (Roche). Supernatants of culture media were collected 48–60 hours after transfection and centrifuged at 82,700 × g to concentrate the lentivirus. The pellet was resuspended in PBS, aliquoted, and frozen at −80°C. To transduce hippocampal or cortical neurons, 10–20 μl of concentrated viral supernatant was used for each 6 well dish.

Biotinylation assay of surface-expressed receptors

Primary cultured neurons were biotinylated with 1 mg/ml EZ-Link Sulfo-NHS-SS-biotin as previously described47. Neurons were then harvested in hypotonic lysis buffer (10 mM HEPES-OH, pH 7.4, 10 mM KCl, 0.1 mM EDTA, EDTA-free complete protease inhibitor), sonicated briefly, and sedimented by centrifugation at 100,000 × *g* for 20 min. In Figure 3f, neurons were homogenized using 20 strokes with a glass homogenizer and passed through a 23 G needle ten times. Sucrose was then added to a final concentration of 0.32 M. Nuclear pellet was removed by centrifugation at 800 × *g* for 5 min, and the supernatant was collected and centrifuged at 10,000 × *g* for 20 min to obtain crude synaptosome P2 pellet. The pellet was resuspended in lysis buffer without Triton X-100, solubilized with 1% SDS with final concentration for 10 min at 37 °C, and then 2% Triton X-100 were added to the lysate resulting in a final concentration of 0.2% SDS. After insoluble material was removed, surface-expressed receptors were isolated as previously described47. The data were quantified by measuring surface receptor to total receptor band intensity ratios using ImageJ software and normalizing to control cultures from at least three independent experiments.

Recycling assay of internalized receptors

A recycling assay to measure recycled NMDA receptors of internalized pools in primary hippocampal neurons was modified from a previous report29. Primary hippocampal neurons (DIV 5) were transduced with lentivirus harboring scrambled or SNAP-23 shRNA. N-terminal tagged GFP-NR2B was transfected into the infected neurons at DIV12 using Lipofectamine 2000 reagent (Invitrogen). 36–48 hours after transfection, the hippocampal neurons were incubated with rabbit anti-GFP antibody (1: 500, Invitrogen) at RT for 10 min and then incubated at 37°C for 30 min to allow internalization of receptors. Non-internalized surface bound antibody was then blocked with excess of unconjugated anti-rabbit IgG Fab at RT for 20 min. Neurons were then incubated at 37 °C for 1 hour to allow recycling back to the plasma membrane. Surface recycled receptors, and internalized receptors, were labeled as previously described47. Briefly, neurons were fixed and incubated for 30 min with Alexa 647-conjugated anti-rabbit secondary antibody to label the recycled surface population of receptors before permeabilization. After permeabilization, neurons were incubated with Alexa 568-conjugated anti-rabbit secondary antibody to label the internalized population of receptors. Individual color signals were converted as shown on images in Figure 5. Control experiments confirmed that the fluorescence signal from GFP-NR2B was insignificant as compared to the EGFP fluorescence of the lentiviral vector. The amount of recycling was quantitated using MetaMorph 7.5 software (Universal Imaging Corp., Downingtown, PA). Data for internalized receptor are presented as the percentage of the internalized fraction as compared to the total (surface + internalized) fraction. Data for recycled receptor are presented as the percentage of surface (recycled) fraction as compared to the total

(internalized + recycled) fraction. Statistical significance was determined using a Student's unpaired *t* test.

Lentiviral expression of shRNA in cultured hippocampal slices and electrophysiology

Techniques were as described previously48. Briefly, hippocampal slices were prepared from 1 week old rats and following 1 hour of recovery, lentivirus was pressure ejected into part of the CA1 cell body region. Slices were placed in culture for 7–10 days after which time they were used for electrophysiology. Whole cell patch-clamp recordings were made from CA1 pyramidal neurons using standard techniques. Infected neurons were identified by GFP fluorescence and uninfected neurons were used as in-slice controls. The extracellular solution during recordings was as follows (mM): 125 NaCl, 3.25 KCl, 1.25 $NaHPO_4$, 25 $NaHCO_3$, 4 $CaCl_2$, 4 $MgSO_4$, 10 glucose, 0.1 picrotoxin, 0.002 2-chloroadenosine, saturated with 95% O_2/ 5% CO_2. The following intracellular solution was used for whole-cell recordings (mM): 135 $CsMeSO_4$, 8 NaCl, 10 HEPES, 0.5 EGTA, 4 Mg-ATP, 0.3 Na-GTP, 1–5 QX-314, 0.6 Na-phosphocreatine, 0.1 spermine, pH 7.2, 285–290 mOsm. EPSCs were evoked by electrical stimulation of axons in *stratum radiatum* at a frequency of 0.2 Hz. For analysis of synaptic NMDA receptors, the NMDA component of the mixed AMPA and NMDA receptor-mediated EPSC at a holding potential of +40 mV was measured between 70 ms and 90 ms after the peak of the EPSC. Data were collected using Axopatch 200B or Multicalmp 700A amplifiers (Axon Instruments), filtered at 5 kHz and digitised at 10 kHz. EPSC amplitude, DC current, input resistance and series resistance were continuously monitored on-line. Recordings were terminated if series resistance deviated by more than 20%.

Supplementary Material

Refer to Web version on PubMed Central for supplementary material.

Acknowledgements

We thank Dr. Ya-Xian Wang for help with the immunogold labeling, John D. Badger II for preparing primary neuron cultures, and Dr. Mikyoung Park (Stanford University) for helpful technical comments. We also thank the NINDS Light Imaging Facility, in particular the help of Dr. Carolyn Smith. In addition, we would like to acknowledge the NINDS sequencing facility. This research was supported by the NCI Intramural Research Program (P.A.R.), the NINDS Intramural Research Program (Y.H.S. and K.W.R.), the Integrative Neural Immune Program (Y.H.S. fellowship), and the intramural program of the NIDCD (R.S.P. and R.J.W.).

References

1. Mayer A. Membrane fusion in eukaryotic cells. Annu. Rev. Cell Dev. Biol. 2002; 18:289–314. [PubMed: 12142286]
2. Jahn R, Sudhof TC. Membrane fusion and exocytosis. Annu. Rev. Biochem. 1999; 68:863–911. [PubMed: 10872468]
3. Jahn R, Scheller RH. SNAREs - engines for membrane fusion. Nat. Rev. Mol. Cell Biol. 2006; 7:631–643. [PubMed: 16912714]
4. Lin RC, Scheller RH. Mechanisms of synaptic vesicle exocytosis. Annu. Rev. Cell Dev. Biol. 2000; 16:19–49. [PubMed: 11031229]
5. Duc C, Catsicas S. Ultrastructural localization of SNAP-25 within the rat spinal cord and peripheral nervous system. J. Comp. Neurol. 1995; 356:152–163. [PubMed: 7629308]

6. Oyler GA, et al. The identification of a novel synaptosomal-associated protein, SNAP-25, differentially expressed by neuronal subpopulations. J. Cell Biol. 1989; 109:3039–3052. [PubMed: 2592413]
7. Tao-Cheng JH, Du J, McBain CJ. Snap-25 is polarized to axons and abundant along the axolemma: an immunogold study of intact neurons. J. Neurocytol. 2000; 29:67–77. [PubMed: 11068335]
8. Washbourne P, et al. Genetic ablation of the t-SNARE SNAP-25 distinguishes mechanisms of neuroexocytosis. Nat. Neurosci. 2002; 5:19–26. [PubMed: 11753414]
9. Ravichandran V, Chawla A, Roche PA. Identification of a novel syntaxin- and synaptobrevin/VAMP-binding protein, SNAP-23, expressed in non-neuronal tissues. J. Biol. Chem. 1996; 271:13300–13303. [PubMed: 8663154]
10. Chen D, Bernstein AM, Lemons PP, Whiteheart SW. Molecular mechanisms of platelet exocytosis: role of SNAP-23 and syntaxin 2 in dense core granule release. Blood. 2000; 95:921–929. [PubMed: 10648404]
11. Foster LJ, Yaworsky K, Trimble WS, Klip A. SNAP23 promotes insulin-dependent glucose uptake in 3T3-L1 adipocytes: possible interaction with cytoskeleton. Am. J. Physiol. Cell Physiol. 1999; 276:C1108–C1114.
12. Guo Z, Turner C, Castle D. Relocation of the t-SNARE SNAP-23 from lamellipodia-like cell surface projections regulates compound exocytosis in mast cells. Cell. 1998; 94:537–548. [PubMed: 9727496]
13. Vaidyanathan VV, Puri N, Roche PA. The last exon of SNAP-23 regulates granule exocytosis from mast cells. J. Biol. Chem. 2001; 276:25101–25106. [PubMed: 11350976]
14. Bragina L, et al. Heterogeneity of glutamatergic and GABAergic release machinery in cerebral cortex. Neuroscience. 2007; 146:1829–1840. [PubMed: 17445987]
15. Chen D, Minger SL, Honer WG, Whiteheart SW. Organization of the secretory machinery in the rodent brain: distribution of the t-SNAREs, SNAP-25 and SNAP-23. Brain Res. 1999; 831:11–24. [PubMed: 10411979]
16. Verderio C, et al. SNAP-25 modulation of calcium dynamics underlies differences in GABAergic and glutamatergic responsiveness to depolarization. Neuron. 2004; 41:599–610. [PubMed: 14980208]
17. Sadoul K, et al. SNAP-23 is not cleaved by botulinum neurotoxin E and can replace SNAP-25 in the process of insulin secretion. J. Biol. Chem. 1997; 272:33023–33027. [PubMed: 9407084]
18. Lau CG, Zukin RS. NMDA receptor trafficking in synaptic plasticity and neuropsychiatric disorders. Nat. Rev. Neurosci. 2007; 8:413–426. [PubMed: 17514195]
19. Wenthold RJ, Prybylowski K, Standley S, Sans N, Petralia RS. Trafficking of NMDA receptors. Annu. Rev. Pharmacol. Toxicol. 2003; 43:335–358. [PubMed: 12540744]
20. Groc L, Choquet D. AMPA and NMDA glutamate receptor trafficking: multiple roads for reaching and leaving the synapse. Cell Tissue Res. 2006; 326:423–438. [PubMed: 16847641]
21. Roche KW, et al. Molecular determinants of NMDA receptor internalization. Nat. Neurosci. 2001; 4:794–802. [PubMed: 11477425]
22. Lavezzari G, McCallum J, Dewey CM, Roche KW. Subunit-specific regulation of NMDA receptor endocytosis. J. Neurosci. 2004; 24:6383–6391. [PubMed: 15254094]
23. Sans N, et al. NMDA receptor trafficking through an interaction between PDZ proteins and the exocyst complex. Nat. Cell Biol. 2003; 5:520–530. [PubMed: 12738960]
24. Washbourne P, Liu XB, Jones EG, McAllister AK. Cycling of NMDA receptors during trafficking in neurons before synapse formation. J. Neurosci. 2004; 24:8253–8264. [PubMed: 15385609]
25. Tovar KR, Westbrook GL. Mobile NMDA receptors at hippocampal synapses. Neuron. 2002; 34:255–264. [PubMed: 11970867]
26. Oyler GA, Polli JW, Wilson MC, Billingsley ML. Developmental expression of the 25-kDa synaptosomal-associated protein (SNAP-25) in rat brain. Proc. Natl. Acad. Sci. USA. 1991; 88:5247–5251. [PubMed: 1711221]
27. Vaidyanathan VV, Roche PA. Structure and chromosomal localization of the mouse SNAP-23 gene. Gene. 2000; 247:181–189. [PubMed: 10773458]

28. Cahill AL, Herring BE, Fox AP. Stable silencing of SNAP-25 in PC12 cells by RNA interference. BMC Neurosci. 2006; 7:9. [PubMed: 16445859]
29. Scott DB, Michailidis I, Mu Y, Logothetis D, Ehlers MD. Endocytosis and degradative sorting of NMDA receptors by conserved membrane-proximal signals. J. Neurosci. 2004; 24:7096–7109. [PubMed: 15306643]
30. Sutton RB, Fasshauer D, Jahn R, Brunger AT. Crystal structure of a SNARE complex involved in synaptic exocytosis at 2.4 angstrom resolution. Nature. 1998; 395:347–353. [PubMed: 9759724]
31. Leung SM, Chen D, DasGupta BR, Whiteheart SW, Apodaca G. SNAP-23 requirement for transferrin recycling in Streptolysin-O-permeabilized Madin-Darby canine kidney cells. J. Biol. Chem. 1998; 273:17732–17741. [PubMed: 9651373]
32. Lledo PM, Zhang X, Sudhof TC, Malenka RC, Nicoll RA. Postsynaptic membrane fusion and long-term potentiation. Science. 1998; 279:399–403. [PubMed: 9430593]
33. Nishimune A, et al. NSF binding to GluR2 regulates synaptic transmission. Neuron. 1998; 21:87–97. [PubMed: 9697854]
34. Osten P, et al. The AMPA receptor GluR2 C terminus can mediate a reversible, ATP-dependent interaction with NSF and alpha- and beta-SNAPs. Neuron. 1998; 21:99–110. [PubMed: 9697855]
35. Song I, et al. Interaction of the N-ethylmaleimide-sensitive factor with AMPA receptors. Neuron. 1998; 21:393–400. [PubMed: 9728920]
36. Lan JY, et al. Protein kinase C modulates NMDA receptor trafficking and gating. Nat. Neurosci. 2001; 4:382–390. [PubMed: 11276228]
37. Lan JY, et al. Activation of metabotropic glutamate receptor 1 accelerates NMDA receptor trafficking. J. Neurosci. 2001; 21:6058–6068. [PubMed: 11487629]
38. Luscher C, et al. Role of AMPA receptor cycling in synaptic transmission and plasticity. Neuron. 1999; 24:649–658. [PubMed: 10595516]
39. Selak S, et al. A role for SNAP25 in internalization of kainate receptors and synaptic plasticity. Neuron. 2009; 63:357–371. [PubMed: 19679075]
40. Hayashi T, et al. Synaptic vesicle membrane fusion complex: action of clostridial neurotoxins on assembly. EMBO J. 1994; 13:5051–5061. [PubMed: 7957071]
41. Petralia RS, Sans N, Wang YX, Wenthold RJ. Ontogeny of postsynaptic density proteins at glutamatergic synapses. Mol. Cell. Neurosci. 2005; 29:436–452. [PubMed: 15894489]
42. Petralia RS, Wang YX, Wenthold RJ. Internalization at glutamatergic synapses during development. Eur. J. Neurosci. 2003; 18:3207–3217. [PubMed: 14686895]
43. Petralia RS, Wenthold RJ. Immunocytochemistry of NMDA receptors. Methods Mol. Biol. 1999; 128:73–92. [PubMed: 10320974]
44. Yi Z, et al. The role of the PDZ protein GIPC in regulating NMDA receptor trafficking. J. Neurosci. 2007; 27:11663–11675. [PubMed: 17959809]
45. Carlin RK, Grab DJ, Cohen RS, Siekevitz P. Isolation and characterization of postsynaptic densities from various brain regions: enrichment of different types of postsynaptic densities. J. Cell Biol. 1980; 86:831–845. [PubMed: 7410481]
46. Schluter OM, Xu W, Malenka RC. Alternative N-terminal domains of PSD-95 and SAP97 govern activity-dependent regulation of synaptic AMPA receptor function. Neuron. 2006; 51:99–111. [PubMed: 16815335]
47. Suh YH, et al. Corequirement of PICK1 binding and PKC phosphorylation for stable surface expression of the metabotropic glutamate receptor mGluR7. Neuron. 2008; 58:736–748. [PubMed: 18549785]
48. Terashima A, et al. An essential role for PICK1 in NMDA receptor-dependent bidirectional synaptic plasticity. Neuron. 2008; 57:872–882. [PubMed: 18367088]

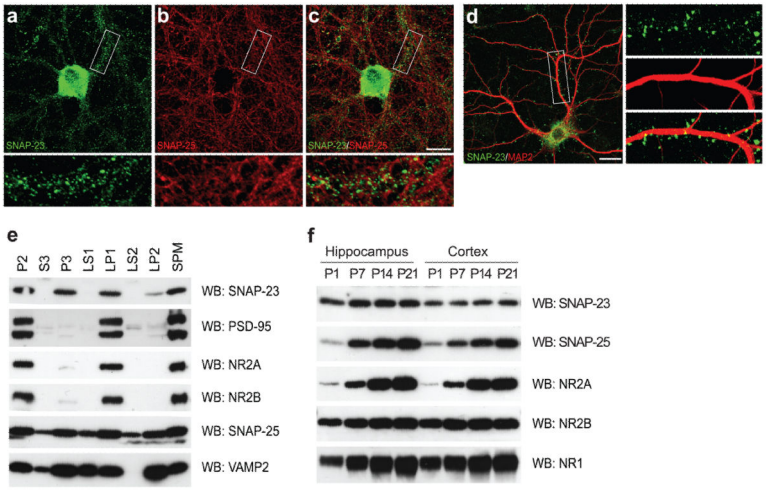

Figure 1. SNAP-25 and SNAP-23 are differentially expressed in neurons

(**a**–**c**) Hippocampal neurons were labeled with purified rabbit SNAP-23 and mouse monoclonal SNAP-25 antibodies as indicated. Alexa 488 anti-rabbit secondary antibody was used to visualize endogenous SNAP-23 (**a**) and Alexa 568 anti-mouse secondary antibody for SNAP-25 (**b**). Merged images are shown (**c**). Images were collected with a confocal immunofluorescence microscope with 60 × objective and maximal projections are shown as described in the Methods. The lower panels show higher magnification images of the individual processes boxed in the upper panel images. Scale bar, 20 μm. (**d**) Hippocampal neurons were labeled with SNAP-23 and mouse MAP2 antibodies. Alexa 488 secondary antibody was used to visualize SNAP-23 and Alexa 568 secondary antibody for MAP2. Scale bar, 20 μm. (**e**) Subcellular fractionation reveals that the distribution of SNAP-23 differs from that of SNAP-25. Twenty micrograms of protein from each subcellular fraction were loaded and immunoblotted as indicated. P2, crude synaptosomal fraction; S3, cytosolic fraction; P3, microsomal membrane fraction; LS1, synaptic vesicle and cytosolic supernatant fraction; LP1, synaptosomal membrane fraction; LS2, synaptosomal-cytosolic fraction; LP2, crude synaptic vesicle-enriched fraction; SPM, synaptic plasma membrane. (**f**) Developmental expression of SNAP-23 in brain. Crude synaptosomes (P2 fraction) from mouse hippocampus or cortex were solubilized and subjected to immunoblottings with the indicated antibodies.

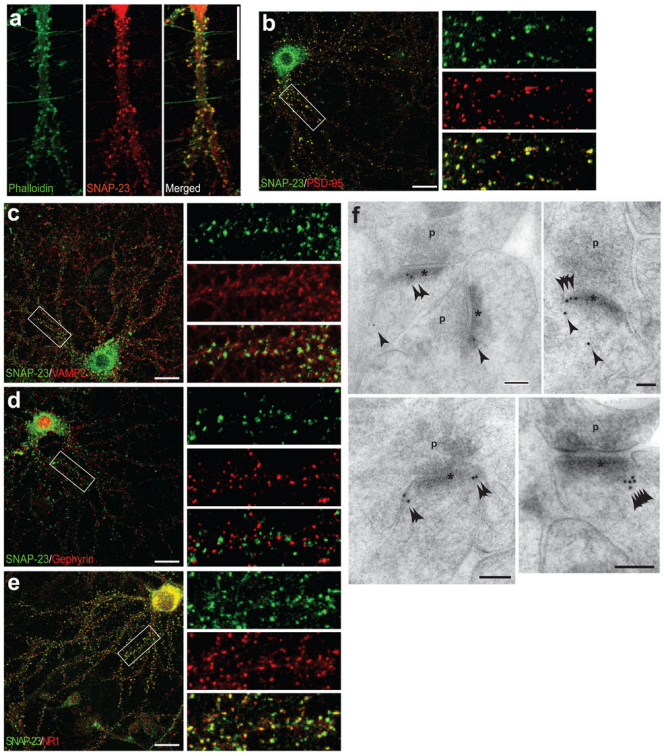

Figure 2. Endogenous SNAP-23 is enriched at excitatory synapses on dendritic spines

(**a**) Hippocampal neurons were stained with purified rabbit anti-SNAP-23 and anti-rabbit Alexa 568 secondary antibody, followed by a 5 min incubation with Phalloidin-Alexa 488 to visualize F-actin. Scale bar, 20 μm. (**b**–**e**) Hippocampal neurons were labeled with rabbit SNAP-23 antibody and mouse monoclonal PSD-95, Synaptobrevin/VAMP-2, Gephyrin, or NR1 antibodies as indicated. Alexa 488 anti-rabbit secondary antibody was used to visualize endogenous SNAP-23 and Alexa 568 anti-mouse secondary antibody for PSD-95 (**b**), Synaptobrevin/VAMP-2 (**c**), Gephyrin (**d**), and NR1 (**e**). Panels show higher-magnification images of the individual processes boxed in the larger images on the left. Scale bars, 20 μm. (**f**) Immunogold electron microscopy labeling of endogenous SNAP-23. Gold particles (arrowheads) label endogenous SNAP-23 in postsynaptic spines in the CA1 stratum radiatum. p, presynaptic terminal; asterisk, PSD. Scale bars, 100 nm.

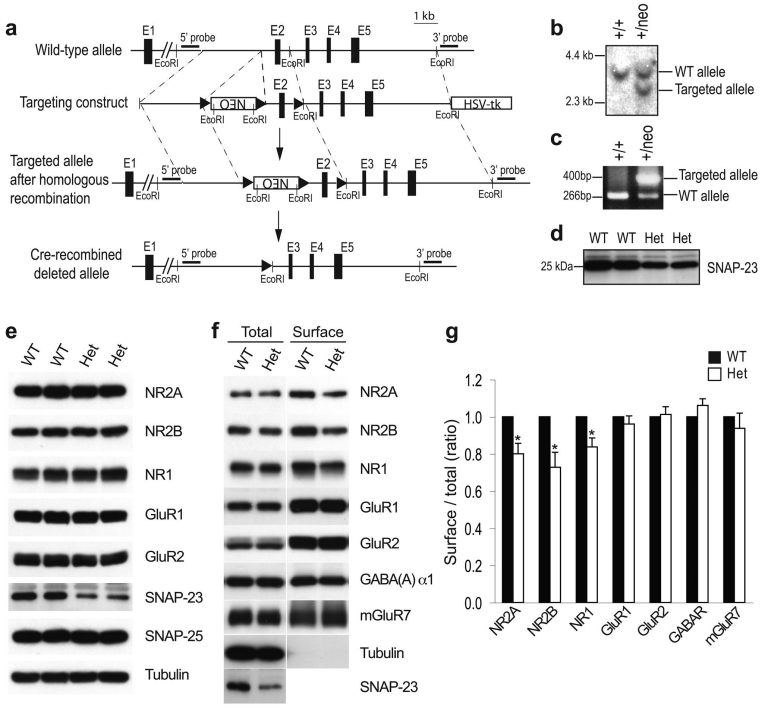

Figure 3. NMDA receptor surface expression is reduced in SNAP-23 heterozygous mice

(**a**) Targeting strategy to remove *Snap-23* exon 2 (E2) containing the initiator ATG. The structures of the wild-type *Snap-23* gene and the targeting construct are shown. Exons E1 to E5 are represented as black boxes. Using a genomic clone harboring the *Snap-23* gene, a targeting vector containing the neomycin resistance gene flanked by loxP sites and the TK gene was generated. Following homologous recombination in ES cells, targeted heterozygous mice containing targeted allele were obtained. Mice harboring the *Snap-23* E2-deleted allele were generated by breeding with EIIa-Cre transgenic mice. (**b**) Southern blot analysis of genomic DNA isolated from tails of *Snap-23* E2-targeted mice. EcoRI-digested genomic DNA was hybridized with the 5′ probe. (**c**) Genomic PCR to detect the targeted and wild-type alleles from tail DNA of E2-targeted mice. (**d**) Expression of SNAP-23 was analyzed by immunoblotting whole brain lysates of SNAP-23 heterozygous (Het) mice and wild-type (WT) littermates. (**e**) Expression of glutamate receptors in the P2 crude synaptosome fraction from hippocampus of SNAP-23 Het and WT littermates. (**f**) Surface expression of glutamate receptors was analyzed using a surface biotinylation assay in primary cortical neurons from SNAP-23 Het and WT littermates. Surface receptors were isolated by precipitation using Streptavidin-agarose beads and immunoblotted with the indicated antibodies. (**g**) Quantitation of the immunoblots was performed by measuring the band intensity of the biotinylated fraction compared with the intensity of total input using ImageJ software. Graphs represent means ± s.e.m. *p<0.01 (n = 3–5) (p=0.0077 for NR2A, 0.0097 for NR2B, 0.0095 for NR1, 0.4130 for GluR1, 0.7772 for GluR2, 0.1706 for GABA(A) α1, and 0.4740 for mGluR7).

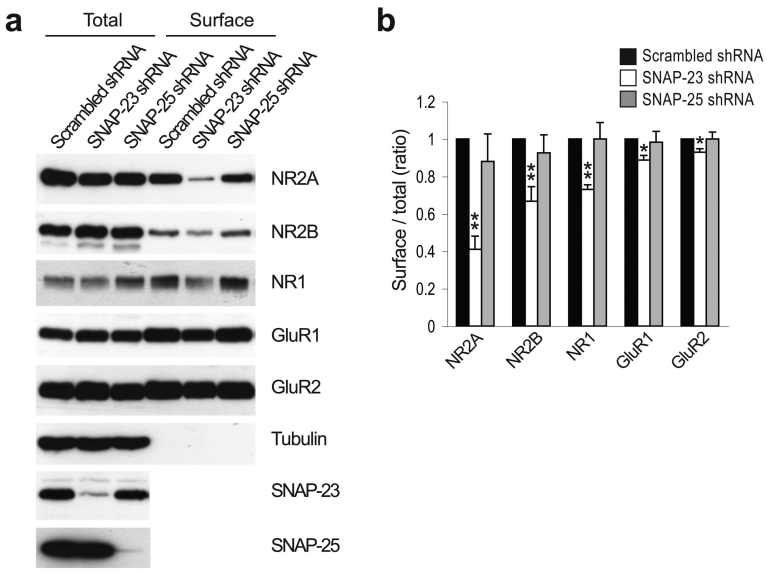

Figure 4. SNAP-23, but not SNAP-25, regulates surface expression of NMDA receptors

(**a**) Primary hippocampal neurons (DIV 5–7) were transduced with scrambled, SNAP-23, or SNAP-25 shRNA lentivirus for 7 days. Surface expression of glutamate receptors was evaluated using a surface biotinylation assay. (**b**) Quantitation of the immunoblots was performed by measuring the band intensity of the biotinylated fraction compared with the band intensity of total input using ImageJ software. Graphs represent means ± s.e.m. **p<0.01, *p<0.05 (n = 5) [p=0.0004 (NR2A), 0.0078 (NR2B), 0.0004 (NR1), 0.0103 (GluR1), 0.0176 (GluR2) for SNAP-23 shRNA; p=0.4526 (NR2A), 0.4727 (NR2B), 0.9965 (NR1), 0.7723 (GluR1), 0.9977 (GluR2) for SNAP-25 shRNA compared with scrambled shRNA].

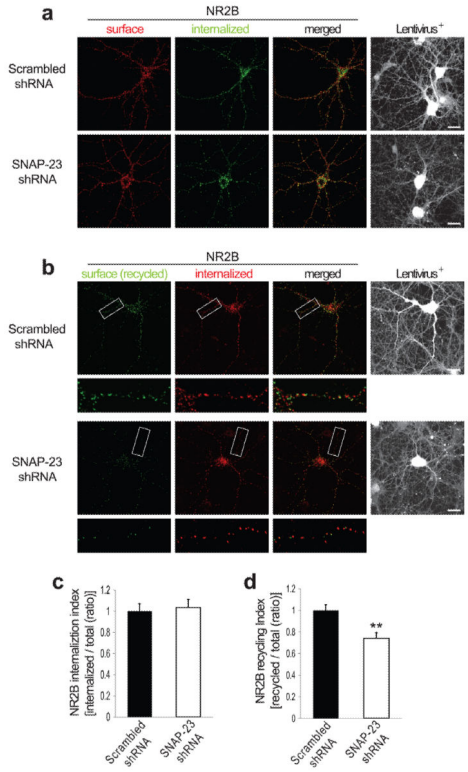

Figure 5. SNAP-23 regulates the recycling of the NMDA receptor subunit NR2B

Internalization (**a**) and recycling (**b**) of NR2B-containing NMDA receptors. Scrambled or SNAP-23 shRNA lentivirus-transduced primary hippocampal neurons were transfected with GFP-NR2B at DIV12. Surface, internalized, and recycled receptor populations were labeled as described in the Methods. The lower panels show higher magnification images of the individual processes boxed in the upper panel images. Scale bars, 20 μm. (**c**) Internalized receptors (panel a) are presented as the percentage of internalized compared to total (surface + internalized) fraction. Graphs represent means ± s.e.m. $p>0.05$ ($n > 45$ neurons from 3 independent experiments) ($p= 0.5709$). (**d**) Recycled receptors (panel b) are presented as the percentage of recycled receptor compared to total (internalized + recycled) fraction. Graphs represent means ± s.e.m. $^{**}p<0.01$ ($n > 60$ neurons from 4 independent experiments) ($p=0.009$).

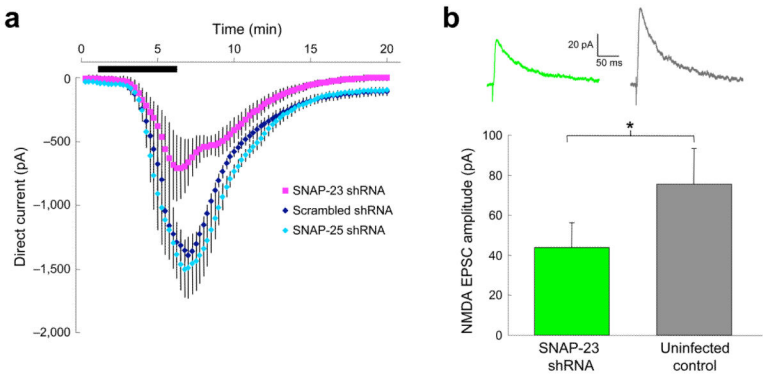

Figure 6. Knock-down of SNAP-23 causes a reduction in NMDA-evoked currents and NMDA EPSCs in CA1 pyramidal neurons

(**a**) Mean amplitude of direct current recorded from voltage-clamped CA1 pyramidal neurons in cultured hippocampal slices at a holding potential of −40 mV in response to a 5 min bath application of NMDA (50 μM; indicated by black bar) for cells expressing SNAP-23 shRNA, SNAP-25 shRNA or scrambled shRNA (n = 8 for all). Peak inward current in SNAP-23 shRNA cells is significantly reduced compared to scrambled shRNA ($p<0.05$). (**b**) Mean amplitude of NMDA EPSCs evoked in CA1 pyramidal neurons expressing SNAP-23 shRNA and from in-slice uninfected control neurons at a holding potential of +40 mV using the same stimulus position and intensity (n = 6, *$p<0.05$). Inset top: example traces.